Coupled channel effects for the charmed-strange mesons

Wei Hao,[1,2,*] Yu Lu,[2,†] and Bing-Song Zou[1,2,3,‡]

[1]*CAS Key Laboratory of Theoretical Physics, Institute of Theoretical Physics, Chinese Academy of Sciences, Beijing 100190, China*

[2]*School of Physical Sciences, University of Chinese Academy of Sciences (UCAS), Beijing 100049, China*

[3]*School of Physics and Electronics, Central South University, Changsha 410083, China*

(Received 24 August 2022; accepted 3 October 2022; published 14 October 2022)

We make a systematic calculation of the spectra and hadronic decays of the D_s system in a coupled channel framework, where the unquenched effects are induced by the $^3P_0$ model. In the calculation, the wave functions are obtained by using a nonrelativistic potential model and are handled precisely with Gaussian expansion method. Even though the fitting mainly focuses on the spectrum, our model agrees well with the experiments on both the spectra and the hadronic decays, suggesting that the coupled channel effect could result in a reasonable and coherent description of the D_s mesons. Based on the calculation, we give a detailed analysis on various aspects of the excited states, especially $D_{s0}^*(2317)$, $D_{s1}(2460), D_{s1}(2536), D_{s1}^*(2860), D_{s0}(2590)$, and $D_{sJ}^*(3040)$. We also predict that $D_{s0}^*(2^3P_0)$ should be a D^*K^* dominant molecule with mass 2894 MeV, which is only 5 MeV below the D^*K^* threshold.

DOI: 10.1103/PhysRevD.106.074014

I. INTRODUCTION

Back in 1964, in order to build a schematic model of baryons and mesons, Gell-Mann [1] and independently Zweig [2] proposed a fundamental component now called quarks to be the building blocks of hadrons. In this model, baryons and mesons are compounds of three quarks and quark-antiquark pairs, respectively. This breakthrough lays the playground for the development of quantum chromodynamics (QCD), which is widely believed to be the fundamental theory of strong interactions. However, due to the asymptotic freedom of the QCD, the coupling constant becomes comparable to one around ∼300 MeV, making the perturbation calculation approach infeasible.

Two general frameworks at the quark level have been proposed to circumvent this difficulty. One way is the lattice QCD, where the space-time is discretized and the QCD is simulated on supercomputers. Another way belongs to various QCD-inspired phenomenological models.

Within the phenomenological model approach, and an elaborate treatment of the relativistic effect from the gluon, Godfrey and Isgur [3] construct a sophisticate potential and demonstrate that the conventional quark model (CQM) or quenched quark model can explain a wide range of properties of hadrons, from the spectra to the decay widths, light mesons to heavy quarkonia. This relativistic model is now known as GI model and was later applied to baryons [4]. and with the newly observed data, the parameters are also refitted for $D_{(s)}$ and $B_{(s)}$ mesons [5,6].

Although the GI model is a big achievement, it cannot be the whole story even on the theoretical side, since the contributions of the fluctuation caused by sea quarks are totally ignored. An additional mechanism has to be added in order to describe the hadronic decay process. This static picture is also challenged by the experimental measurements. For D_s system, even though the ground state, such as $^1S_0$ and $^3S_1$, are well reproduced by a quenched quark model [3], higher charmed-strange mesons are still not well understood.

In 2003, the discovery of $D_{s0}^*(2317)$ [7] and $D_{s1}(2460)$ [8] has stimulated a lot of discussions. The two particles are peculiar by their unexpected low masses and narrow widths compared to the quark model predictions [3]. Many theoretical interpretations have been proposed to address the discrepancy, including the CQM with modification to the potential of GI model [9], hadronic molecules, and compact tetraquark states [10–15].

The challenge to the CQM does not stop. Recently, a new excited D_s^+ meson named $D_{s0}(2590)$ was observed in $B^0 \to D^-D^+K^+\pi^-$ decay by LHCb Collaboration using a data sample corresponding to an integrated luminosity of

*haowei2020@itp.ac.cn
†ylu@ucas.ac.cn
‡zoubs@itp.ac.cn

5.4 fb^{-1} at a center-of-mass energy of 13 TeV [16]. The mass, total decay width, and spin parity were detected to be $m = 2591 \pm 6 \pm 7$ MeV, $\Gamma = 89 \pm 16 \pm 12$ MeV, and $J^P = 0^-$, respectively. This state was predicted to be $D_{s0}(2^1S_0)$ with mass 2673 MeV [3] by the relativistic quark model, 2646 MeV by the screen potential model [17], and 2640 MeV by the nonrelativistic quark model [18]. All these predictions overestimate its mass by 50–80 MeV. There are also works to interpret it as the $D_{s0}(2^1S_0)$ state with D^*K component [19,20] in the coupled-channel framework. For reviews on these mesons, see Refs. [21,22] and references therein.

Although there are numerous works on D_s mesons, the coupled-channel effects (CCEs) still remain to be further explored. On the side of calculation method, simple harmonic oscillator approximation of the wave function is still widely used although accurate methods are available such as the Gaussian expansion method (GEM) [23]. On the theoretical side, it is common that special attention is paid to near threshold states, such as $D^*_{s0}(2317)$, or that hadronic decay widths and spectra are often separately discussed or restrained to excited D_s mesons. This may due to the fact that unquenched quark model (UQM), such as GI model, is quite successful on low lying states. However, as will be shown in this paper, the achievement on the low-lying states of the CQM does not mean that low-lying states are free from the CCEs and it is more reasonable to treat all the states in a unified way.

Moreover, for the D_s mesons, the mass gap between $D_s(1968)$ and the DK threshold is less than 400 MeV. This value is much smaller than the case of the bottomonium $[m(B\bar{B}) - m(\eta_b(1S)) \approx 1160$ MeV] or even the charmonium $m(D\bar{D}) - m(\eta_c(1S)) \approx 760$ MeV, which is a strong hint of a sizable CCE. Since it has been shown by Li *et al.* that some effect can be absorbed into the potential in UQM [24], the parameters in UQM should be refitted if the CCEs are calculated in a self-consistent approach.

A systematic research of UQM for the bottomonium has been done in Ref. [25]. However, it remains unanswered as to whether it is possible to explain various properties of D_s mesons with UQM, where CCEs are estimated to be large. In this work, instead of fitting the lowest spectra in the CQM and only switch on the CCEs for the near-threshold states, we perform the fitting in a fully-coupled channel approach, where the mass shift from CCEs are consistently treated for all D_s mesons. Other ingredients of CCEs are also coherently discussed, such as hadronic decays and renormalization of wave functions.

This paper is organized as follows. In Sec. II, we explain the calculation framework of coupled channel effects, the details of $^3P_0$ model and the quenched model. Section III is devoted to the analysis of the results of our coupled channel calculation with various detailed comparisons and elucidation of D_s mesons. Finally, we give a short summary of this work in Sec. IV.

II. THEORETICAL FORMALISM

A. Nonrelativistic quark model

The quenched part of the Hamiltonian H_A is taken from the a potential model where α_s^2 correction is explicitly addressed. This model was proposed by Lakhina and Swanson [9], and has been used to study the bottom mesons [26] and open charm mesons [18]. The Hamiltonian H_A can be split into a term H_0 which could be solved nonperturbatively and a spin-dependent term H_{sd} which we solve in leading-order perturbation theory,

$$H_A = H_0 + H_{sd}, \tag{1}$$

$$H_0 = m_q + m_{\bar{q}} + \frac{\nabla^2}{2M_r} - \frac{4}{3}\frac{\alpha_s}{r} + br + C_{q\bar{q}} + \frac{32\alpha_s\sigma^3 e^{-\sigma^2 r^2}}{9\sqrt{\pi}m_q m_{\bar{q}}}\boldsymbol{S}_q \cdot \boldsymbol{S}_{\bar{q}}, \tag{2}$$

where M_r is the reduced mass of which equals to $M_r = m_q m_{\bar{q}}/(m_q + m_{\bar{q}})$. When combined together with the subscript, $\boldsymbol{S}$ and m stand for the spin and mass of quark or antiquark, respectively. where $m_q, m_{\bar{q}}, \alpha_s, b, C_{q\bar{q}}$, and σ are the free parameters we need to refit in this quenched model.

The H_{sd} can be compressed as

$$H_{sd} = \left(\frac{\boldsymbol{S}_q}{2m_q^2} + \frac{\boldsymbol{S}_{\bar{q}}}{2m_{\bar{q}}^2}\right)\cdot\boldsymbol{L}\left(\frac{1}{r}\frac{dV_c}{dr} + \frac{2}{r}\frac{dV_1}{dr}\right) + \frac{\boldsymbol{S}_+\cdot\boldsymbol{L}}{m_q m_{\bar{q}}}\left(\frac{1}{r}\frac{dV_2}{r}\right) + \frac{3\boldsymbol{S}_q\cdot\hat{\boldsymbol{r}}\boldsymbol{S}_{\bar{q}}\cdot\hat{\boldsymbol{r}} - \boldsymbol{S}_q\cdot\boldsymbol{S}_{\bar{q}}}{3m_q m_{\bar{q}}}V_3 + \left[\left(\frac{\boldsymbol{S}_q}{m_q^2} - \frac{\boldsymbol{S}_{\bar{q}}}{m_{\bar{q}}^2}\right) + \frac{\boldsymbol{S}_-}{m_q m_{\bar{q}}}\right]\cdot\boldsymbol{L}V_4, \tag{3}$$

where

$$\begin{aligned}
V_c &= -\frac{4}{3}\frac{\alpha_s}{r} + br,\\
V_1 &= -br - \frac{2}{9\pi}\frac{\alpha_s^2}{r}[9\ln(\sqrt{m_q m_{\bar{q}}}r) + 9\gamma_E - 4],\\
V_2 &= -\frac{4}{3}\frac{\alpha_s}{r} - \frac{1}{9\pi}\frac{\alpha_s^2}{r}[-18\ln(\sqrt{m_q m_{\bar{q}}}r) + 54\ln(\mu r) + 36\gamma_E + 29],\\
V_3 &= -\frac{4\alpha_s}{r^3} - \frac{1}{3\pi}\frac{\alpha_s^2}{r^3}[-36\ln(\sqrt{m_q m_{\bar{q}}}r) + 54\ln(\mu r) + 18\gamma_E + 31],\\
V_4 &= \frac{1}{\pi}\frac{\alpha_s^2}{r^3}\ln\left(\frac{m_{\bar{q}}}{m_q}\right),
\end{aligned} \tag{4}$$

where $\boldsymbol{S}_\pm = \boldsymbol{S}_q \pm \boldsymbol{S}_{\bar{q}}$, $\boldsymbol{L}$ is the orbital angular momentum of the $q\bar{q}$ system. γ_E is Euler constant, C_F and C_A are gauge

group factors, and μ is renormalization scale. The value of the parameters are taken from Ref. [9]; $\gamma_E = 0.5772$, $C_F = 4/3$, $C_A = 3$ and $\mu = 1$ GeV.

The spin-orbit term in the H_{sd} can be rewritten into the symmetric part $H_{\rm sym}$ and the antisymmetric part $H_{\rm anti}$,

$$H_{\rm sym} = \frac{\boldsymbol{S}_+ \cdot \boldsymbol{L}}{2}\left[\left(\frac{1}{2m_q^2}+\frac{1}{2m_{\bar{q}}^2}\right)\left(\frac{1}{r}\frac{dV_c}{dr}+\frac{2}{r}\frac{dV_1}{dr}\right) + \frac{2}{m_q m_{\bar{q}}}\left(\frac{1}{r}\frac{dV_2}{r}\right)+\left(\frac{1}{m_q^2}-\frac{1}{m_{\bar{q}}^2}\right)V_4\right], \tag{5}$$

$$H_{\rm anti} = \frac{\boldsymbol{S}_- \cdot \boldsymbol{L}}{2}\left[\left(\frac{1}{2m_q^2}-\frac{1}{2m_{\bar{q}}^2}\right)\left(\frac{1}{r}\frac{dV_c}{dr}+\frac{2}{r}\frac{dV_1}{dr}\right) + \left(\frac{1}{m_q^2}+\frac{1}{m_{\bar{q}}^2}+\frac{2}{m_q m_{\bar{q}}}\right)V_4\right]. \tag{6}$$

The antisymmetric part $H_{\rm anti}$ gives rise to the spin-orbit mixing of the mesons, such as $D_s(n^3L_L) - D_s(n^1L_L)$. This mixing can be parametrized by a mixing angle θ_{nL} by the following formula [3,27],

$$\begin{pmatrix} D_{sL}(nL) \\ D'_{sL}(nL) \end{pmatrix} = \begin{pmatrix} \cos\theta_{nL} & \sin\theta_{nL} \\ -\sin\theta_{nL} & \cos\theta_{nL} \end{pmatrix}\begin{pmatrix} D_s(n^1L_L) \\ D_s(n^3L_L) \end{pmatrix}, \tag{7}$$

where $D_{sL}(nL)$ and $D'_{sL}(nL)$ represent the physical observed states.

B. $^3P_0$ model and coupled channel effects

In the coupled channel framework, the full Hamiltonian is defined as

$$H = H_A + H_{BC} + H_I, \tag{8}$$

where H_A is the Hamiltonian of the quark-antiquark pairs. In this work, we adopt a nonrelativistic potential model whose detailed form is discussed in the next subsection. H_{BC} is the Hamiltonian between the meson pairs, which we called BC pairs

$$H_{BC} = E_{BC} = \sqrt{m_B^2 + p^2} + \sqrt{m_C^2 + p^2}. \tag{9}$$

H_I is the term which induce the mixing between $q\bar{q}$ bare state and BC meson pair system. In this work, we use the widely used $^3P_0$ model [28–30], where the generated quark-antiquark pairs are assumed to share the same quantum numbers with the vacuum $J^{PC} = 0^{++}$. This assumption results in the conclusion that the spin and orbital-angular momentum to be both 1, thus the spectroscopy notation $^{2S+1}L_J$ of the system reads $^3P_0$.

The quark-antiquark pair-creation operator $T^\dagger$ is expressed as [31–33]

$$T^\dagger = -3\gamma_0^{\rm eff}\int d\vec{p}_3 d\vec{p}_4 \delta(\vec{p}_3+\vec{p}_4) C_{34} F_{34} e^{-r_q^2(\vec{p}_3-\vec{p}_4)^2/6} \times [\chi_{34}\times \mathcal{Y}_1(\vec{p}_3-\vec{p}_4)]_0^{(0)} b_3^\dagger(\vec{p}_3) d_4^\dagger(\vec{p}_4), \tag{10}$$

where C_{34}, F_{34}, and χ_{34} are the color-singlet wave function, flavor-singlet wave function, and spin-triplet wave function of the $q\bar{q}$ respectively. $b_3^\dagger(\vec{p}_3)$ and $d_4^\dagger(\vec{p}_4)$ are the creation operators for a quark and an antiquark with momenta $\vec{p}_3$ and $\vec{p}_4$, respectively. $\gamma_0^{\rm eff} = \frac{m_n}{m_i}\gamma_0$ is the pair-creation strength, whose value is obtained by fitting the strong decay of the $D_{s2}^*(2573)$ (1^3P_2). m_n refers to the light quark mass m_u, and m_i refers to the quark mass m_u, m_d, or m_s. In the $^3P_0$ model, the operator $T^\dagger$ creates a pair of constituent quarks with an actual size, the pair-creation point has to be smeared out by a Gaussian factor, whose width r_q was determined from meson decays to be in the range 0.25 0.35 fm [34–37]. In our calculation, we take the value $r_q = 0.3$ fm.

The eigenfunction of the full Hamiltonian H can be expressed as

$$|\psi\rangle = c_0|\psi_0\rangle + \sum_{BC}\int d^3p\, c_{BC}(p)|BC;p\rangle, \tag{11}$$

where c_0 is the normalization constant before the $q\bar{q}$ bare state. $c_{BC}(p)$ is the normalization constant with specific momentum p for BC molecular components.

Meanwhile, the eigenvalue M of H in Eq. (8) is the theoretical prediction of the coupled channel model which can be decomposed into two terms [38],

$$M = M_0 + \Delta M \tag{12}$$

$$\Delta M = \sum_{BC}\int_0^\infty p^2 dp \frac{|\langle BC;p|T^\dagger|\psi_0\rangle|^2}{M - E_{BC} + i\epsilon}, \tag{13}$$

where M_0 is the eigenvalue of the quenched Hamiltonian H_A and ΔM is the mass shift which signifies the deviation between H and H_A. If the initial state A is above the threshold of B and C, a strong decay process $A \to BC$ will happen and ΔM will pick up a imaginary part which is equal to one half of the decay width.

$$\Gamma_{BC} = 2\pi p_0 \frac{E_B(p_0)E_C(p_0)}{m_A}|\langle BC;p_0|T^\dagger|\psi_0\rangle|^2. \tag{14}$$

For states below the BC threshold, it is reasonable to normalize the physical state $|\psi\rangle$, and the probability of quenched quark pairs can be calculated as

$$P_{q\bar{q}} \equiv |c_0|^2 = \left(1 + \sum\nolimits_{BC}\int_0^\infty p^2 dp \frac{|\langle BC;p\ell J|T^\dagger|\psi_0\rangle|^2}{(M-E_{BC})^2}\right)^{-1}, \tag{15}$$

and the probability of the molecular component are naturally expressed as $P_{BC} = 1 - P_{q\bar{q}}$. For D_s mesons, BC is often represented by various coupled channels, such as DK or $D_s\eta$. We also use P_{molecule} to represent the sum of all the coupled-channel probabilities. If the states are located above the threshold, it is not possible to normalize the wave functions. However, we can still estimate the proportion of the closed channel by

$$P_{BC} \equiv \int d^3p |c_{BC(p)}|^2 = \int_0^\infty p^2 dp \frac{|\langle BC; p|T^\dagger|\psi_0\rangle|^2}{(M - E_{BC})^2}, \tag{16}$$

which is equivalent to fix $P_{q\bar{q}} = 1$. When the probabilities is expressed in this form, it is convenient to estimate and compare the proportion of different components. In this work, we adopt the assumption that the opened channels contribution to the wave functions can be discarded [39], which will make the normalization proceed.

As can be seen from above, the occurrence of H_I will not only result in a mass shift ΔM to the spectrum and a decay process but also renormalize the wave function. These three effects are jointly called coupled channel effects (CCEs) which we aim to explore in the next section. For other aspects of the CCEs like $S - D$ mixing, we encourage the readers to Ref. [25].

III. RESULTS AND DISCUSSIONS

After solving the Schrödinger equation with Hamiltonian H_0, the wave functions are used to determine the leading order correction of H_{sd} in the quenched quark model and the CCEs to the spectrum and strong decays and wave functions.

The refitted parameters are listed in Table I. They are fixed by fitting the strong decay of the $D^*_{s2}(2573)$ and the spectrum of $D_s(1^1S_0)$, $D^*_s(1^3S_1)$, $D^*_{s0}(2317)(1^3P_0)$, $D^*_{s2}(2573)(1^3P_2)$, $D^*_{s3}(2860)(1^3D_3)$, $D_{s0}(2590)(2^1S_0)$, and $D^*_{s1}(2700)(2^3S_1)$, and all the input values are taken from PDG [40]. We also list these parameters from the previous quark model. That indicates that the coupled channel effects can cause the difference.

With the above fitting parameters, we get the following mixing angles in Eq. (7) to be $-29.5°$, $-32.7°$, and $-41.9°$ for $1P$, $2P$, and $1D$, respectively. In the screened potential model the mixing angle could be $-42.7°$, $-31.4°$, and $-39.4°$ [41]. In the quenched quark model it could be $-24.5°$, $-32.3°$, and $-40.2°$ [18]. Although the exact numbers for the mixing angles in various quark models are different, they are close. Results on the spectrum are shown in Fig. 1 with numbers listed in Table II.

A general conclusion is that all the D_s mesons contain sizable molecular components, among which, D^*K^* contributes dominantly. This large contribution is mainly due to the spin-enhancement effect.

TABLE I. Parameters refitted in this work.

Parameter	This work	Ref. [18]
m_n	0.419 GeV	0.45 GeV
m_s	0.569 GeV	0.55 GeV
m_c	1.464 GeV	1.43 GeV
α_s	0.6072	0.5
b	0.1314 GeV^2	0.14 GeV^2
σ	1.2071 GeV	1.17 GeV
C_{cs}	0.1381 GeV	−0.325 GeV
γ_0	0.529	0.452

For states below DK thresholds, the wave function of D_s mesons can be normalized, and our calculation shows that even the ground state 1^1S_0, which is widely accepted as a pure $c\bar{s}$ in the quenched picture, contains 17% molecular components. As we explained in the Introduction, the DK threshold is much lower for D_s mesons, and this result verifies what we have anticipated; the CCEs are important for the study of the D_s mesons, even for the ground states.

We need to point out that even though the CQM have the ability to reproduce the spectrum, this does not mean that CQM is an good approximation for the ground state D_s mesons. The achievement of CQM on ground state is mainly due to the fact that the CCEs can be partially absorbed into the parameters. e.g., the constant term in the potential can be leveraged to absorb the mass shift in CCEs. However, as we have discussed in the previous section, the mass shift only reflects one aspect of the CCEs. For other impacts in CCEs, like the renormalization of the wave functions, there is no way to embrace it in the CQM since it is conceptually beyond the CQM.

The breakdown of the CQM can also be revealed by the famous $D^*_{s0}(2317)$ and $D_{s1}(2460)$. The CQM-like GI model [5] predict their masses to be 167 MeV and 89 MeV higher, respectively. As a comparison, with CCEs consistently calculated, our results agrees excellently with the PDG results. Since the decay channel DK above $D^*_{s0}(2317)$

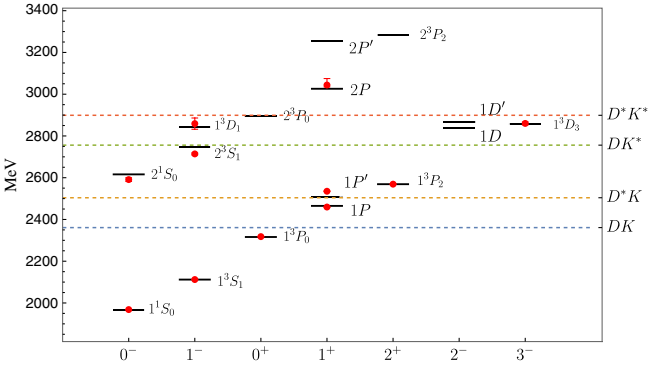

FIG. 1. The spectrum of the D_s mesons. Red dots with error bars denote the experimental values from PDG [40] and our calculations are depicted as black lines.

TABLE II. The mass spectrum (in MeV) of the $c\bar{s}$ mesons. Columns 3 to 5 stand for spectrum from the potential model, the mass shift, and the spectrum with coupled channel effects, respectively. Results from Ref. [18] are listed in column 6 as a comparison. The last column contains the experimental values taken from PDG [40].

$n^{2S+1}L_J$	State	M_0	ΔM	M	NR [18]	PDG [40]
1^1S_0	D_s	2272	−304	1968	1969	1968.34 ± 0.07
1^3S_1	D_s^*	2472	−359	2112	2107	2112.2 ± 0.4
2^1S_0	$D_{s0}(2590)$	2989	−373	2616	2640	$2591 \pm 6 \pm 7$ [16]
2^3S_1	$D_{s1}^*(2700)$	3081	−334	2747	2714	2714 ± 5
1^3P_0	$D_{s0}^*(2317)$	2668	−351	2316	2344	2317.8 ± 0.5
$1P$	$D_{s1}(2460)$	2843	−378	2465	2488	2459.5 ± 0.6
$1P'$	$D_{s1}(2536)$	2897	−392	2506	2510	2535.11 ± 0.06
1^3P_2	$D_{s2}^*(2573)$	2959	−390	2569	2559	2569.1 ± 0.8
2^3P_0	–	3151	−257	2894	2830	–
$2P$	$D_{sJ}^*(3040)$	3302	−276	3026	2958	3044^{+31}_{-9}
$2P'$	–	3367	−112	3255	2995	–
2^3P_2	–	3422	−138	3283	3040	–
1^3D_1	$D_{s1}^*(2860)$	3159	−315	2843	2804	2859 ± 27
$1D$	–	3175	−336	2839	2788	–
$1D'$	–	3216	−350	2866	2849	–
1^3D_3	$D_{s3}^*(2860)$	3206	−350	2855	2811	2860 ± 7

and as a $J^P = 1^+$ particle, $D_{s1}(2460)$ cannot decay to two 0^- final state. The only allowed hadronic decay is the isospin symmetry-breaking process $D_s^* \to D_s\pi$, resulting a narrow width for both.

The mixing between $D_{s1}(2460)$ and $D_{s1}(2536)$ are assumed to be caused by the antisymmetric part in the spin-orbit Hamiltonian H_{anti}, and with our fitted parameters, the mixing angle is predicted to be $-29.5°$. As can be seen from Table II, our prediction of $D_{s1}(2460)$ is only 5 MeV above the experimental central value.

A noticeable deviation is the mass of $D_{s1}(2536)$, our prediction is about 30 MeV lighter than the PDG averaged value. However, this result could be improved within the coupled channel framework, since an additional off-diagonal term which represents the mixing between bare state and the molecular state will enlarge the mass gap between $1P$ and $1P'$, thus lifting the mass of $1P'$ to be closer to the experimental measures. This requires a refitting of all the parameters and we postpone this challenge for later work.

TABLE III. Probabilities (in %) of the coupled channels considered in this work. For the convenience of comparison, values from columns 3 to 12 (various coupled channels) are rescaled by $P_{c\bar{s}}$, such that $P_{c\bar{s}} = 100\%$. e.g., for $D_{s0}^*(2317)$, $P_{c\bar{s}} : P_{DK} = 100 : 45.5$ "–" means that the corresponding channel is open and its contribution to the wave function normalization is discarded, see the discussion below Eq. (15). $P_{c\bar{s}}$ and P_{molecule} represent the probability of the $c\bar{s}$ and the summation of the probability of all the coupled channels, respectively.

$(n_r+1)^{2S+1}L_J$	State	DK	DK^*	D^*K	D^*K^*	$D_s\eta$	$D_s\eta'$	$D_s\phi$	$D_s^*\eta$	$D_s^*\eta'$	$D_s^*\phi$	P_{molecule}	$P_{c\bar{s}}$
1^1S_0	D_s	0.0	4.3	3.5	8.5	0.0	0.0	1.1	0.7	0.2	2.2	17.0	83.0
1^3S_1	D_s^*	2.5	4.2	3.8	13.9	0.4	0.1	1.0	0.7	0.2	3.5	23.2	76.8
1^3P_0	$D_{s0}^*(2317)$	45.5	0.0	0.0	19.9	1.7	0.2	0.0	0.0	0.0	4.2	40.3	59.7
$1P$	$D_{s1}(2460)$	0.0	8.5	42.8	19.1	0.0	0.0	1.3	1.8	0.3	3.8	43.7	56.3
$1P'$	$D_{s1}(2536)$	–	10.8	–	17.9	–	–	1.7	1.9	0.4	3.4	26.5	73.5
1^3P_2	$D_{s2}^*(2573)$	–	8.5	–	22.8	–	0.2	1.4	1.2	0.3	4.0	27.7	72.3
2^1S_0	$D_{s0}(2590)$	–	20.4	–	26.2	–	–	2.0	4.1	0.4	3.7	36.2	63.8
2^3S_1	$D_{s1}^*(2700)$	–	51.3	–	47.3	–	0.2	1.6	–	0.3	4.7	51.3	48.7
1^3D_1	$D_{s1}^*(2860)$	–	–	–	47.6	–	0.5	0.6	–	0.1	5.8	35.3	64.7
$1D$	–	–	–	–	35.4	–	–	2.0	–	0.4	4.1	29.5	70.5
$1D'$	–	–	–	–	46.9	–	–	2.3	–	0.4	3.9	34.9	65.1
1^3D_3	$D_{s3}^*(2860)$	–	–	–	54.4	–	0.2	1.4	–	0.3	3.8	37.5	62.5
2^3P_0	–	–	–	–	167.5	–	0.6	–	–	–	4.0	63.2	36.8

The probabilities of each coupled channel are listed in column 3–12 in Table III, where $P_{c\bar{s}}$ is set to 1 for comparison convenience. One general feature is that P_{molecule} is not negligible even for the ground state D_s mesons. This may explain why it is a challenge to fit the spectrum in CQM because of the universal CCEs.

Another impact of the Table III is that 40.3% of $D^*_{s0}(2317)$ is made up of various molecular components and the dominant DK molecule is 27.2%. $D_{s1}(2460)$ contains a larger molecular components (43.7%) where dominant component becomes D^*K (24.1%). The large molecular components also offers a partial reason as to why it is difficult to incorporate them in the quenched-quark model.

For states above the threshold, the additional quark pairs leads to hadronic decay. As can be seen from Table IV, our prediction on the hadronic decay widths agree excellently with the experimental measurement, given that our fit focuses mainly on the spectrum and the only hadronic decay with in the fitting is that of $D^*_{s2}(2573)$.

For $D^*_{s1}(2700)$, our result 2747 MeV is more close to the newly LHCb measurement $2732.3 \pm 4.3 \pm 5.8$ MeV [42] instead of the PDG averaged 2714 ± 5 MeV, and its molecular components could be as large as 51.3%. This also challenges the assignment that $D^*_{s1}(2700)$ is a good candidate of pure 2^3S_1. This result can be further improved when $^3S_1 - {}^3D_1$ mixing introduced by CCEs is considered. Additionally, because a cross-term in the Hamiltonian will increase the mass splitting, this $S-D$ mixing also have the potential to improve our result of $D^*_{s1}(2860)$. Since the mass uncertainties of $D^*_{s1}(2860)$ is still relatively large, and $S-D$ mixing is not the center of this work, we postpone the study of the fine structure to later work.

As the name suggest, $D^*_{s1}(2860)$ and $D^*_{s3}(2860)$ are nearly equally heavy with each other. Although the GI model predicts a small mass splitting between $D^*_{s1}(1^3D_1)$ and $D^*_{s3}(1^3D_3)$ [5], the claimed masses are 40–60 MeV heavier than experimental results. As a comparison, our results reproduce the spectra very well. Furthermore, our calculation not only reproduces the total decay widths of both particles, but also matches the branch ratio of $\Gamma(D_s(2860) \to D^*K)/\Gamma(D_s(2860) \to DK)$. The ratios are around 0.9 for both $D^*_{s1}(2860)$ and $D^*_{s3}(2860)$, which agrees with the measurement from *BABAR* [43] $(1.10 \pm 0.15 \pm 0.19)$.

For $D^*_{sJ}(3040)$, the total decay width also matches the experimental measured values [43] $239 \pm 35^{+46}_{-42}$ MeV and our calculation suggests that the main decay channel is D^*K^*. Since the main decay channel of K^* is $K^* \to K\pi$, we suggest to search at the channel $D^*K\pi$ to verify our prediction.

One important prediction in this work is about the property of $D^*_{s0}(2^3P_0)$. Our calculation shows that its mass is 2894 MeV, only 5 MeV below D^*K^* threshold. This value is 111 MeV below the GI Model prediction [5]. The hadronic width is 47 MeV and it decays mainly to DK. It also couples strongly to D^*K^*, and as suggested in Table III, this coupling is around 1.7 times as large as that of the $c\bar{s}$ core. This exceedingly large coupling concludes that around 62% of 2^3P_0 consists of the D^*K^* molecule, which is quite beyond the conventional quark model, and we suggest searching for related signals experimentally.

TABLE IV. The decay widths of the $2S$, $1P$, $2P$ and $1D$ states. "–" means no experimental information or the strong decay is forbidden.

Channel		Width	Exp.
2^1S_0	$D_{s0}(2590)$	112	$89 \pm 16 \pm 12$ [16]
2^3S_1	$D^*_{s1}(2700)$	114	122 ± 10
1^3P_0	$D^*_{s0}(2317)$	–	<3.8
$1P$	$D_{s1}(2460)$	–	<3.5
$1P'$	$D_{s1}(2536)$	0.4	0.92 ± 0.05
1^3P_2	$D^*_{s2}(2573)$	17	16.9 ± 0.7
2^3P_0	–	47	–
$2P$	$D^*_{sJ}(3040)$	279	239 ± 60
$2P'$	–	331	–
2^3P_2	–	421	–
1^3D_1	$D^*_{s1}(2860)$	110	159 ± 80
$1D$	–	145	–
$1D'$	–	106	–
1^3D_3	$D^*_{s3}(2860)$	67	53 ± 10

IV. SUMMARY

We made a coupled channel calculation of the D_s mesons, where the spectrum and the decay width are coherently calculated. The decent match with the experiment on the spectra, decay widths, or even the decay branch ratios gives us a strong evidence that the coupled channel effects are able to explain both the ground and the excited D_s mesons. We get universally sizable non-$c\bar{s}$ components for all the D_s mesons, which also signifies a strongly coupled channel effect. The large non-$c\bar{s}$ component offers a natural explanation why some excited D_s mesons are "exotic" for quenched potential models.

$D^*_{s0}(2317)$ and $D_{s1}(2460)$ can be nicely explained in this framework. Our results show that they have 40.3% and 43.7% non-$c\bar{s}$ components, respectively. For $D_{s1}(2536)$, our calculation also agrees with the experiment that the decay width is quite small. For the two $1D$ states, our predicted spectra, 2843 MeV for D^*_{s1} and 2855 MeV for D^*_{s3} also agree with experimental measurements. Their strong decay patterns differs most at channel DK^*. $\Gamma(D^*_{s1} \to DK^*)$ is 35 MeV which is around ten times larger than that of D^*_{s3}. We also predict the masses of the unobserved D_{s2} mesons to be between 2788 MeV and 2849 MeV.

Another prediction is related to $D^*_{s0}(2^3P_0)$. We claim that the bare $D^*_{s0}(2^3P_0)$ should mix considerably with D^*K^*, and the relative percentage after mixing is

$P_{c\bar{s}}:P_{D^*K^*}=1:1.675$. We predict its mass should be 2894 MeV with decay width 47 MeV and the dominant decay channel is DK (41 MeV).

ACKNOWLEDGMENTS

The authors are grateful to Feng-kun Guo and Jia-jun Wu for valuable suggestions and comments. This work is supported by the NSFC and the Deutsche Forschungsgemeinschaft (DFG, German Research Foundation) through the funds provided to the Sino-German Collaborative Research Center TRR110 Symmetries and the Emergence of Structure in QCD (NSFC Grant No. 12070131001, DFG Project-ID No. 196253076-TRR 110), by the NSFC Grants No. 11835015 and No. 12047503, and by the Chinese Academy of Sciences (CAS) under Grant No. XDB34030000.

APPENDIX: MASS SHIFT AND DECAY WIDTH OF EACH COUPLED CHANNEL

In this appendix we give the mass shift and decay width of each channel. The concrete values are listed in Tables V–VII.

TABLE V. Mass shift ΔM (in MeV) of each coupled channel.

State	DK	DK^*	D^*K	D^*K^*	$D_s\eta$	$D_s\eta'$	$D_s\phi$	$D_s^*\eta$	$D_s^*\eta'$	$D_s^*\phi$	Total
1^1S_0	0	−61	−43	−130	0	0	−17	−10	−4	−39	−304
1^3S_1	−19	−48	−35	−176	−4	−1	−13	−8	−3	−53	−359
2^1S_0	0.0	−77	−88	−149	0	0	−14	−11	−3	−32	−373
2^3S_1	2	−70	−13	−194	−2	−1	−9	−9	−2	−37	−334
1^3P_0	−62	0	0	−222	−6	−2	0	0	0	−59	−351
$1P$	0	−56	−68	−183	0	0	−13	−9	−3	−47	−378
$1P'$	0	−75	−89	−156	0	0	−17	−11	−4	−39	−392
1^3P_2	−37	−59	−49	−172	−5	−2	−13	−8	−3	−42	−390
2^3P_0	−3	0	0	−217	−3	−1	0	0	0	−33	−257
$2P$	0	−33	−8	−195	0	0	−7	−4	−2	−27	−276
$2P'$	0	−16	−28	−20	0	0	−8	−3	−3	−34	−112
2^3P_2	−19	−22	−30	−23	−3	−1	−4	−3	−2	−32	−138
1^3D_1	13	−19	4	−257	0.3	−1	−2	−2	−1	−52	−315
$1D$	0	−75	−24	−180	0	0	−11	−8	−2	−36	−336
$1D'$	0	−83	−41	−168	0	0	−14	−9	−3	−31	−350
1^3D_3	−28	−60	−45	−164	−5	−1	−10	−7	−2	−29	−350

TABLE VI. The decay widths of the $2S$ and $1P$ states. "−" means the channel is forbidden.

	2^1S_0	2^3S_1	1^3P_0	$1P$	$1P'$	1^3P_2
Channel	$D_{s0}(2590)$	$D_{s1}^*(2700)$	$D_{s0}^*(2317)$	$D_{s1}(2460)$	$D_{s1}(2536)$	$D_{s2}^*(2573)$
DK	−	22	−	−	−	15
DK^*	−	−	−	−	−	−
D^*K	112	92	−	−	0.4	2
Total	112	114	−	−	0.4	17
Exp.	$89\pm16\pm12$ [16]	122 ± 10	<3.8	<3.5	0.92 ± 0.05	16.9 ± 0.7

TABLE VII. The decay width of the $2P$ and $1D$ states. "−" means the channel is forbidden or no experimental information.

	2^3P_0	$2P$	$2P'$	2^3P_2	1^3D_1	$1D$	$1D'$	1^3D_3
Channel	−	$D_{sJ}^*(3040)$	−	−	$D_{s1}^*(2860)$	−	−	$D_{s3}^*(2860)$
DK	41	−	−	20	31	−	−	32
DK^*	−	52	12	1	35	99	11	3
D^*K	−	12	8	13	28	45	78	29

(Table continued)

TABLE VII. *(Continued)*

	2^3P_0	$2P$	$2P'$	2^3P_2	1^3D_1	$1D$	$1D'$	1^3D_3
Channel	–	$D_{sJ}^*(3040)$	–	–	$D_{s1}^*(2860)$	–	–	$D_{s3}^*(2860)$
D^*K^*	–	166	197	200	–	–	–	–
$D_s\eta$	5	–	–	1	9	–	–	2
$D_s\eta'$	–	–	–	0.4	–	–	–	–
$D_s\phi$	–	18	21	12	–	–	–	–
$D_s^*\eta$	–	6	7	0.02	5	1	17	1
$D_s^*\eta'$	–	–	1	2	–	–	–	–
$D_s^*\phi$	–	–	41	31	–	–	–	–
$DK_0^*(1430)$	–	–	–	–	–	–	–	–
DK_{1B}	–	–	5	20	–	–	–	–
DK_{1A}	–	–	–	0.2	–	–	–	–
$DK_2^*(1430)$	–	–	–	–	–	–	–	–
$D_0^*(2300)K$	–	3	0.2	–	–	–	0.01	–
$D_1(2420)K$	–	16	3	66	–	–	–	–
$D_1(2430)K$	–	0.03	0.005	9	–	–	–	–
$D_2^*(2460)K$	–	5	38	46	–	–	–	–
Total	47	279	331	421	110	145	106	67
Exp.	–	239 ± 60	–	–	159 ± 80	–	–	53 ± 10

[1] M. Gell-Mann, Phys. Lett. **8**, 214 (1964).
[2] G. Zweig, Report No. CERN-TH-401 (1964), http://cds.cern.ch/record/352337/files/CERN-TH-401.pdf.
[3] S. Godfrey and N. Isgur, Phys. Rev. D **32**, 189 (1985).
[4] S. Capstick and N. Isgur, Phys. Rev. D **34**, 2809 (1986).
[5] S. Godfrey and K. Moats, Phys. Rev. D **93**, 034035 (2016).
[6] S. Godfrey, K. Moats, and E. S. Swanson, Phys. Rev. D **94**, 054025 (2016).
[7] B. Aubert *et al.* (*BABAR* Collaboration), Phys. Rev. Lett. **90**, 242001 (2003).
[8] D. Besson *et al.* (CLEO Collaboration), Phys. Rev. D **68**, 032002 (2003); **75**, 119908(E) (2007).
[9] O. Lakhina and E. S. Swanson, Phys. Lett. B **650**, 159 (2007).
[10] T. Barnes, F. E. Close, and H. J. Lipkin, Phys. Rev. D **68**, 054006 (2003).
[11] Z. Yang, G.-J. Wang, J.-J. Wu, M. Oka, and S.-L. Zhu, Phys. Rev. Lett. **128**, 112001 (2022).
[12] T. E. Browder, S. Pakvasa, and A. A. Petrov, Phys. Lett. B **578**, 365 (2004).
[13] H. J. Lipkin, Phys. Lett. B **580**, 50 (2004).
[14] P. Bicudo, Nucl. Phys. **A748**, 537 (2005).
[15] V. Dmitrasinovic, Phys. Rev. Lett. **94**, 162002 (2005).
[16] R. Aaij *et al.* (LHCb Collaboration), Phys. Rev. Lett. **126**, 122002 (2021).
[17] Q.-T. Song, D.-Y. Chen, X. Liu, and T. Matsuki, Phys. Rev. D **91**, 054031 (2015).
[18] D.-M. Li, P.-F. Ji, and B. Ma, Eur. Phys. J. C **71**, 1582 (2011).
[19] J.-M. Xie, M.-Z. Liu, and L.-S. Geng, Phys. Rev. D **104**, 094051 (2021).
[20] P. G. Ortega, J. Segovia, D. R. Entem, and F. Fernandez, Phys. Lett. B **827**, 136998 (2022).
[21] H.-X. Chen, W. Chen, X. Liu, Y.-R. Liu, and S.-L. Zhu, Rep. Prog. Phys. **80**, 076201 (2017).
[22] H.-X. Chen, W. Chen, X. Liu, Y.-R. Liu, and S.-L. Zhu, arXiv:2204.02649.
[23] E. Hiyama, Y. Kino, and M. Kamimura, Prog. Part. Nucl. Phys. **51**, 223 (2003).
[24] B.-Q. Li, C. Meng, and K.-T. Chao, Phys. Rev. D **80**, 014012 (2009).
[25] Y. Lu, M. N. Anwar, and B.-S. Zou, Phys. Rev. D **94**, 034021 (2016).
[26] Q.-F. Lü, T.-T. Pan, Y.-Y. Wang, E. Wang, and D.-M. Li, Phys. Rev. D **94**, 074012 (2016).
[27] S. Godfrey and R. Kokoski, Phys. Rev. D **43**, 1679 (1991).
[28] L. Micu, Nucl. Phys. **B10**, 521 (1969).
[29] A. Le Yaouanc, L. Oliver, O. Pene, and J. C. Raynal, Phys. Rev. D **8**, 2223 (1973).
[30] A. Le Yaouanc, L. Oliver, O. Pene, and J. C. Raynal, Phys. Rev. D **9**, 1415 (1974).
[31] J. Ferretti, G. Galatà, and E. Santopinto, Phys. Rev. C **88**, 015207 (2013).
[32] J. Ferretti, G. Galata, E. Santopinto, and A. Vassallo, Phys. Rev. C **86**, 015204 (2012).
[33] J. Ferretti and E. Santopinto, Phys. Rev. D **90**, 094022 (2014).

[34] B. Silvestre-Brac and C. Gignoux, Phys. Rev. D **43**, 3699 (1991).
[35] P. Geiger and N. Isgur, Phys. Rev. D **44**, 799 (1991).
[36] P. Geiger and N. Isgur, Phys. Rev. Lett. **67**, 1066 (1991).
[37] P. Geiger and N. Isgur, Phys. Rev. D **55**, 299 (1997).
[38] Y. S. Kalashnikova, Phys. Rev. D **72**, 034010 (2005).
[39] K. Heikkila, S. Ono, and N. A. Tornqvist, Phys. Rev. D **29**, 110 (1984); **29**, 2136(E) (1984).
[40] R. L. Workman (Particle Data Group), Prog. Theor. Exp. Phys. **2022**, 083C01 (2022).
[41] Z. Gao, G.-Y. Wang, Q.-F. Lü, J. Zhu, and G.-F. Zhao, Phys. Rev. D **105**, 074037 (2022).
[42] R. Aaij *et al.* (LHCb Collaboration), J. High Energy Phys. 02 (2016) 133.
[43] B. Aubert *et al.* (*BABAR* Collaboration), Phys. Rev. D **80**, 092003 (2009).